

Controlling Oxidative Addition and Reductive Elimination at Tin(II) via Hemi-Lability

Alexa Caise,^[a] Agamemnon E. Crumpton,^[a] Petra Vasko,^[a,b] Jamie Hicks,^[a] Caitilín McManus,^[a] Nicholas H. Rees,^[a] Simon Aldridge^{*[a]}

[a] Dr. A. Caise, A. Crumpton, Dr. P. Vasko, Dr. J. Hicks, C. McManus, Dr. Nicholas H. Rees, Prof. S. Aldridge
Inorganic Chemistry Laboratory, Department of Chemistry
University of Oxford
South Parks Road, Oxford, OX1 3QR (UK)
E-mail: simon.aldridge@chem.ox.ac.uk

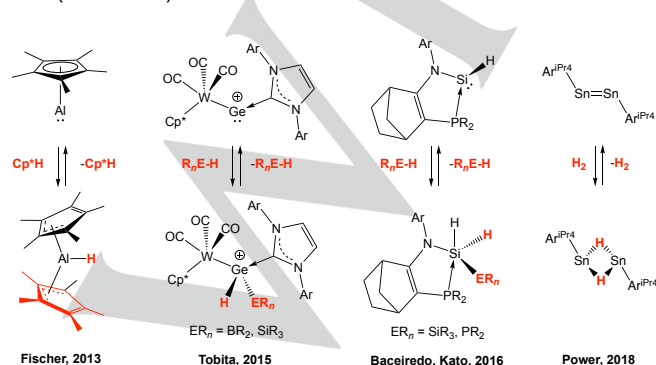
[b] Dr. P. Vasko
Department of Chemistry, Nanoscience Center, University of Jyväskylä
P.O. Box 35, Jyväskylä, Finland, FI-40014

Supporting information for this article is given via a link at the end of the document.

Abstract: We report on the synthesis of a distannyne supported by a pincer ligand bearing pendant amine donors that is capable of reversibly activating E–H bonds at one or both of the tin centres through dissociation of the hemi-labile N–Sn donor/acceptor interactions. This chemistry can be exploited to sequentially (and reversibly) assemble mixed-valence chains of tin atoms of the type $\text{ArSn}(\text{Sn}(\text{Ar})\text{H})_n\text{SnAr}$ ($n = 1, 2$). The experimentally observed (decreasing) propensity towards chain growth with increasing chain length can be rationalized both thermodynamically and kinetically by the electron-withdrawing properties of the $-\text{Sn}(\text{Ar})\text{H}-$ backbone units generated via oxidative addition.

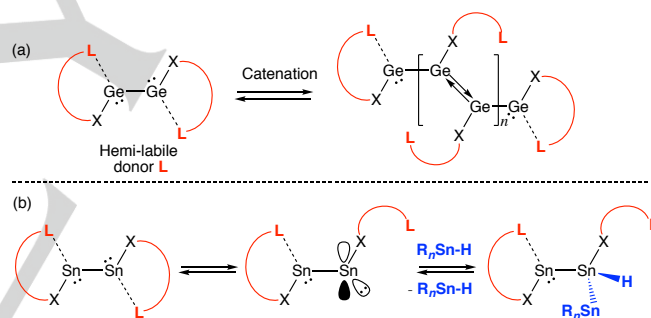
Introduction

Oxidative addition and reductive elimination represent two of the key fundamental steps in synthetic transformations mediated by single-site transition metal catalysts.^[1] Redox reversibility is key to facilitating turnover, and reflects the relatively small potential differences associated with the n and $n+2$ oxidation states for d -block metals. By contrast, main group systems have only very recently begun to find applications in redox-based catalysis.^[2,3] This reflects typically less favourable redox couples, with either the oxidative or reductive step being strongly favoured thermodynamically (depending on the position of the element in the group), and the reverse reaction requiring forcing conditions (such as strongly oxidizing or reducing co-reagents).^[4] As such, examples of main group systems offering favourable energetics (or kinetics) for the reversible activation of E–H bonds are very rare (Scheme 1).^[5,6]



Scheme 1. Selected examples of main group compounds showing reversibility in the activation of E–H bonds.

In recent work we have begun to probe the applications of low-valent main group complexes featuring hemi-labile ancillary donors. Within group 14 chemistry, such ligands offer a means to manipulate access to the reactive metal centres found in two-coordinate metallocenes.^[7] This approach can be exploited to generate extended chains of Ge(I) centres akin to oligo-acetylenes through the formation of Lappert-type double bonds between 'decomplexed' metal centres (Scheme 2a).^[8]



This work: reversible bond activation mediated by (de)coordination of a hemi-labile donor, **L**

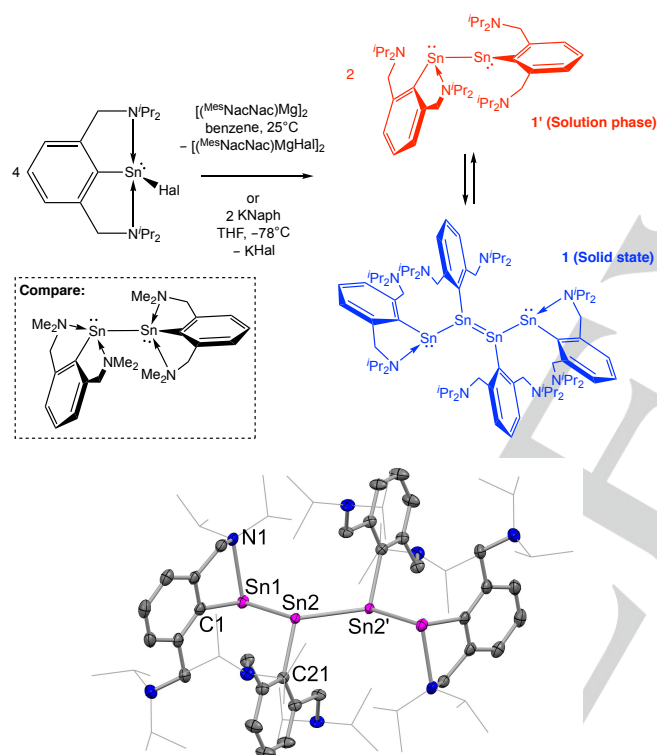
Scheme 2. Exploiting hemi-lability to control access to two-coordinate group 14 metal centres - applications in (a) catenation,^[7] and (b) reversible E–H bond activation.

The coordination of a neutral ancillary donor (such as an amine) is also known to offer a means of modulating main group redox chemistry - for example in promoting (otherwise unfavourable) reductive elimination from Si(IV) to generate base-stabilized Si(II) systems.^[9] With this in mind, we wondered whether a *hemi-labile* ligand scaffold could be exploited to facilitate redox reversibility in bond activation, in particular in the cleavage of E–H bonds by divalent group 14 systems (Scheme 2b). Decoordination of the pendant donor would enable access to a system with appropriate frontier orbitals for E–H oxidative addition,^[4] while re-coordination at divalent E might be expected to promote reductive elimination from a thermodynamic perspective.^[9]

In exploring this hypothesis, we show here that reversibility can be achieved in practice in the activation of Sn–H bonds, and can be exploited to sequentially (and reversibly) assemble mixed-valence chains of tin atoms from a distannyne bearing hemi-labile $-\text{N}^i\text{Pr}_2$ functions.

Results and Discussion

Reduction of $\text{Ar}^{\text{NPr}_2}\text{SnHal}$ ($\text{Hal} = \text{Cl}_{0.6}\text{Br}_{0.4}$, Br, or I; $\text{Ar}^{\text{NR}_2} = \text{C}_6\text{H}_3(\text{CH}_2\text{NR}_2)_2\text{-2,6}$)^[10] with either $[(^{\text{Mes}}\text{NacNac})\text{Mg}]_2$ (0.5 equiv.; $^{\text{Mes}}\text{NacNac} = (\text{NMesCMe})_2\text{CH}$; Mes = 2,4,6- $\text{Me}_3\text{C}_6\text{H}_2$)^[11] in benzene or potassium naphthalenide (KNaph) in THF, followed by recrystallization from Et_2O at -30°C , leads to the formation of a Sn^{I} species of composition $(\text{Ar}^{\text{NPr}_2}\text{Sn})_n$ (Scheme 3). Red/green dichroic crystals can be isolated from diethyl ether, and the product characterised by standard spectroscopic/analytical techniques and by X-ray crystallography. The tetrameric species $(\text{Ar}^{\text{NPr}_2}\text{Sn})_4$ (**1**) present in the solid state closely resembles its germanium counterpart, featuring alternating Sn–Sn single ($d(\text{Sn}(1)\text{--}\text{Sn}(2)/\text{Sn}(1')\text{--}\text{Sn}(2')) = 2.8583(3) \text{ \AA}$)^[12–14] and Sn=Sn double bonds ($d(\text{Sn}(2)\text{--}\text{Sn}(2')) = 2.6909(4) \text{ \AA}$).^[15,16] As with $(\text{Ar}^{\text{NPr}_2}\text{Ge})_4$, the terminal tin atoms (i.e. $\text{Sn}(1)/\text{Sn}(1')$) are coordinated by one of the amino side-arm donors ($d(\text{Sn}(1)\text{--}\text{N}(1)) = 2.421(3) \text{ \AA}$), while the internal tin centres (i.e. $\text{Sn}(2)$) are not coordinated by either *N*-donor (Sn–N contacts of $> 4 \text{ \AA}$).^[7]



Scheme 3. (upper) Synthesis and phase-dependent oligomerization of the distannyne $(\text{Ar}^{\text{NPr}_2}\text{Sn})_2$ **1'**; (lower) Molecular structure of $(\text{Ar}^{\text{NPr}_2}\text{Sn})_4$ (**1**) in the solid state as determined by X-ray crystallography. Solvent molecule and hydrogen atoms omitted, and 'Pr groups shown in wireframe format for clarity. Thermal ellipsoids set at the 40 % probability level. Key bond lengths (Å): Sn1–C1 2.192(4), Sn1–N1 2.421(4), Sn1–Sn2 2.8583(4), Sn2–Sn2' 2.6908(4), Sn2–C21 2.191(4). CCDC ref. 2094340.

In marked contrast to $(\text{Ar}^{\text{NPr}_2}\text{Ge})_4$ (which is intractably insoluble in a range of solvents),^[7] **1** is readily soluble in hydrocarbon media, and has been characterised by ^1H , ^{13}C and ^{119}Sn NMR spectroscopy in benzene- d_6 solution. Moreover, these spectra are not consistent with the solid state structure: a single set of mutually coupled doublets (at $\delta_{\text{H}} = 3.65$ and 3.73 ppm) is observed in the benzylic region of the ^1H NMR spectrum (cf. $\delta_{\text{H}} = 3.29$ and 3.61 ppm for $(\text{Ar}^{\text{NMe}_2}\text{Sn})_2$) and the ^{119}Sn

spectrum features a single resonance at $\delta_{\text{Sn}} = 974 \text{ ppm}$ (cf. $\delta_{\text{Sn}} = 612 \text{ ppm}$ for $(\text{Ar}^{\text{NMe}_2}\text{Sn})_2$ and 793 ppm for $(2,6\text{-Trip}_2\text{C}_6\text{H}_3)\text{SnCl}$ (where Trip = 2,4,6- $\text{Pr}_3\text{C}_6\text{H}_2$)).^[13,17] These data imply that $(\text{Ar}^{\text{NPr}_2}\text{Sn})_4$ dissociates in solution to generate two equivalents of the corresponding distannyne $(\text{Ar}^{\text{NPr}_2}\text{Sn})_2$ (**1'**), with the much lower field ^{119}Sn chemical shift measured for **1'** compared to $(\text{Ar}^{\text{NMe}_2}\text{Sn})_2$, implying significantly weaker coordination of the amine arm(s) in solution.^[18] The minimum energy DFT-calculated structure for **1'** (Scheme 3 and ESI, Figure s22) is unsymmetrical, featuring only one coordinated amine donor arm (cf. four for $(\text{Ar}^{\text{NMe}_2}\text{Sn})_2$; Scheme 3), with the NMR data measured for **1'** at room temperature implying rapid fluxionality on the NMR timescale. Similar dissociation to that observed for **1/1'** in solution is not observed for the germanium analogue $(\text{Ar}^{\text{NPr}_2}\text{Ge})_4$ (presumably due to the stronger nature of the central Ge=Ge bond), but is consistent with trapping of the transient digermynes $(\text{Ar}^{\text{NPr}_2}\text{Ge})_2$ by both Lewis acidic and Lewis basic reagents.

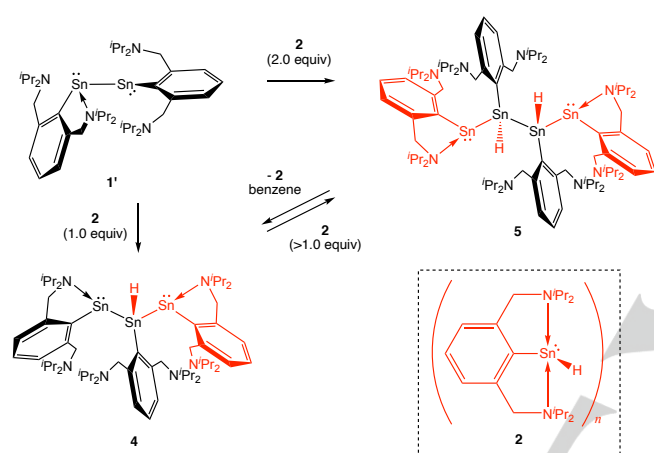
In the case of $(\text{Ar}^{\text{NPr}_2}\text{Sn})_n$, the observed phase-dependent catenation is consistent with the hemi-lability of the pendant NPr_2 donor functions, and with comparable thermodynamic values associated with $\text{N} \rightarrow \text{Sn}$ and $\text{Sn}=\text{Sn}$ bond formation. The contrasting behaviour of $(\text{Ar}^{\text{NMe}_2}\text{Sn})_2$ (dimeric in both solid and solution phases),^[13] emphasizes the role of the steric profile of the *N*-substituents in moderating the strength of the $\text{N} \rightarrow \text{Sn}$ coordinate bond. These experimental findings are consistent with the results of DFT calculations, which suggest that the tetra-tin oligomer $([\text{Ar}^{\text{NR}_2}\text{Sn}]_4)$ and (two equiv. of) the corresponding distannyne $([\text{Ar}^{\text{NR}_2}\text{Sn}]_2)$ are of comparable free energy for $\text{R} = \text{Pr}$ ($\Delta G = -15 \text{ kJ mol}^{-1}$ for dimerization), but that the distannyne is significantly favoured for $\text{R} = \text{Me}$ ($\Delta G = 104 \text{ kJ mol}^{-1}$; see ESI, Table s3).

Given the implied hemi-lability of the pendant amine donors in **1/1'**, we hypothesized that the two-coordinate metal centres might also be accessed for the oxidative activation of E–H bonds at Sn^{I} . Moreover, given the favourable redox chemistry associated with heavier p-block elements,^[19] we postulated that the reverse (reductive elimination) step, might also be feasible, especially if combined with re-coordination of the *N*-donor. As such, this platform might offer a rational approach to reversible bond activation processes. We sought to demonstrate this through the reactions in solution of **1'** with H_2 and with Sn–H bonds.

Tin(II) hydride complex $(\text{Ar}^{\text{NPr}_2}\text{SnH})_n$ (**2**) was prepared by the treatment of $\text{Ar}^{\text{NPr}_2}\text{SnHal}$ with a slight excess of $\text{K}[\text{Et}_3\text{BH}]$ in benzene- d_6 at room temperature (see ESI). The presence of a Sn–H bond in the product is clearly signalled by a resonance at $\delta_{\text{H}} = 11.96 \text{ ppm}$ with ^{119}Sn satellites ($^1J_{\text{SnH}} = 82 \text{ Hz}$), which integrates to 1H. The chemical shift is comparable to those reported for other *N*-donor stabilised tin(II) hydrides, such as $(^{\text{Dipp}}\text{NacNac})\text{SnH}$ ($\delta_{\text{H}} = 13.96 \text{ ppm}$, $^1J_{\text{SnH}} = 64 \text{ Hz}$; $^{\text{Dipp}}\text{NacNac} = (\text{NDippCMe})_2\text{CH}$; Dipp = 2,6- $\text{Pr}_2\text{C}_6\text{H}_3$)^[20] and $[2,6\text{-}\{\text{DippNC}(\text{CH}_3)\}_2\text{C}_6\text{H}_3]\text{SnH}$ ($\delta_{\text{H}} = 10.59 \text{ ppm}$, $^1J_{\text{SnH}} = 112 \text{ Hz}$).^[21] Although **2** could not be obtained as single crystals suitable for X-ray crystallography (due to slow dehydrogenation in hydrocarbon solution - see below), the presence of the tin-bound hydride is further evidenced by hydrometallation of carbon dioxide by **2** to give the corresponding formate complex. Monitoring a solution of **2** in benzene- d_6 by ^1H NMR under ca. 1 bar pressure of CO_2 reveals that it reacts quantitatively at room temperature (within 5 min) to yield $\text{Ar}^{\text{NPr}_2}\text{Sn}(\kappa^2\text{-O}_2\text{CH})$ (**3**), which

has been structurally authenticated by X-ray crystallography (see below). As such, the behaviour of **2** is in line with previous reports of reactivity of tin(II) hydrides with CO₂.^[22,23]

With hydride complex **2** in hand, we set out to examine its reactivity towards distannylene **1'**. Reaction with one equivalent of **1'** in benzene-d₆ was monitored by ¹H NMR spectroscopy, revealing that both reagents are consumed within 5 min to selectively yield a single product. This species is characterized by a singlet resonance at $\delta_{\text{H}} = 5.30$ ppm (with tin satellites; $^1J_{\text{SnH}} = 602$ Hz), and a ¹¹⁹Sn spectrum featuring two resonances: a doublet at $\delta_{\text{Sn}} = -376$ ppm ($^1J_{\text{SnH}} = 602$ Hz), and a broad singlet at $\delta_{\text{Sn}} = 630$ ppm - consistent with the presence of both tetravalent and divalent tin centres.^[18] The molecular structure of the product (**4**) in the solid state was subsequently determined by X-ray crystallography, as the mixed valence tri-tin chain (Ar^{NiPr2}Sn)₃H (Scheme 4 and Figure 1).



Scheme 4. Growth of mixed-valence tri- and tetra-tin chains via Sn-H oxidative addition; inter-conversion of Sn₃ and Sn₄ systems via oxidative addition/reductive elimination.

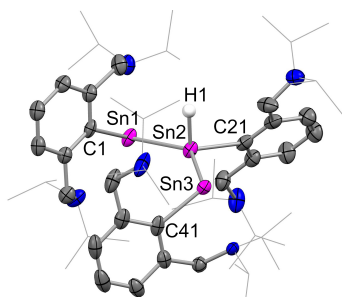
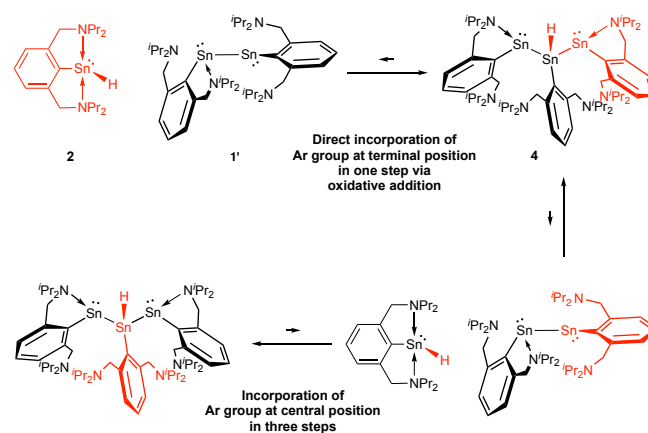


Figure 1. Molecular structure of (Ar^{NiPr2}Sn)₃H (**4**) in the solid state as determined by X-ray crystallography. Solvent molecule and most hydrogen atoms omitted, and Pr groups shown in wireframe format for clarity. Thermal ellipsoids set at the 40 % probability level. Key bond lengths (Å): Sn1–C1 2.186(5), Sn1–N 2.645(6), 2.899(6), Sn1–Sn2 2.930(2), Sn2–C21 2.209(6), Sn2–Sn3 2.921(2), Sn3–C41 2.173(6), Sn3–N 2.604(4), 2.943(7). CCDC ref: 2094342.

The molecular unit of **4** consists of two terminal Ar^{NiPr2}Sn units bound to a central Ar^{NiPr2}SnH moiety, consistent with the structure implied by ¹¹⁹Sn NMR measurements in solution. The hydride ligand was located in the difference Fourier map; its presence was confirmed spectroscopically by an absorption at

1644 cm⁻¹ in the IR spectrum. This stretching frequency is red-shifted relative to those reported for examples of terminal tin(II) hydrides (e.g. (Dipp)₂NacNacSnH, $\nu_{\text{Sn-H}} = 1859$ cm⁻¹; 2,6-{DippNC(CH₃)₂C₆H₃SnH, $\nu_{\text{Sn-H}} = 1826$ cm⁻¹).^[20,21] Both Sn–Sn bond lengths ($d(\text{Sn}(1)\text{--}\text{Sn}(2)) = 2.9304(16)$ Å, $d(\text{Sn}(2)\text{--}\text{Sn}(3)) = 2.9206(11)$ Å) are characteristic of Sn–Sn single bonds, being comparable to those reported for *N*-donor stabilised distannynes.^[13,14] In addition, the two terminal tin centres are characterized by (relatively weak) coordination of one of the amino side-arm donors (e.g. $d(\text{Sn}(1)\text{--}\text{N}(2)) = 2.645(6)$ Å), with the other contact being even longer ($d(\text{Sn}(1)\text{--}\text{N}(1)) = 2.899(6)$ Å), while the central tin atom, Sn(2) is not coordinated by either *N*-donor, with both Sn–N contacts being > 4.7 Å.

The structure of **4** is consistent with its formation from **1'** via oxidative addition of the Sn–H bond of **2** at one of the tin centres of the distannylene, in a manner similar to the mechanism established for the activation of dihydrogen at dimetallynes.^[3a] However, the transformation of **4** to **1'** could also occur through direct insertion of the tin(II) hydride **2** into the Sn–Sn bond of **1'**. Attempts were therefore made to probe the mechanism using NMR-monitored exchange experiments: **4** dissociates to a minor degree in benzene-d₆ solution, generating an equilibrium mixture containing **4** itself (ca. 87 %) and **1'**/2 (ca. 13 %). Chemical exchange between the hydride ligand in **2** and that in **4** can be demonstrated by ¹H NMR saturation transfer experiments. Moreover, the rate of saturation transfer between the two hydride resonances is found to be very similar to the rate of saturation transfer measured for the *para*-CH group of the aryl ligand in **2** and the corresponding *para*-CH signal associated with the terminal Ar^{NiPr2} ligands in **4** (see ESI). These data are consistent with concurrent incorporation of the hydride and aryl ligands from **2** into the hydride and terminal aryl positions of **4**. By contrast, the rate of exchange of the *para*-CH aryl signal of **2** with the *para*-CH signal of the central Ar^{NiPr2} ligand in **4** is slower (by a factor of ≥ 2), consistent with an exchange process which has to occur through successive oxidative addition/reductive elimination/oxidative addition steps (Scheme 5) in order to access the central site. As such, the exchange rate data are consistent with an Sn–H oxidative addition pathway for the formation of **4** from **1'** and **2**.



Scheme 5. Oxidative addition/reductive elimination reactions occurring in the interconversion of **4** and **1'**/2.

With a view to exploring the further potential of this chemistry, and targeting stepwise growth of metal chains via oxidative addition chemistry, we explored the reactivity of **1'** towards further equivalents of **2**. Accordingly, the reaction with two or more equivalents leads to the isolation of the corresponding tetra-tin chain, consisting of two $\text{Ar}^{\text{NiPr}_2}\text{Sn}$ units (at the terminal positions) and two internal $\text{Ar}^{\text{NiPr}_2}\text{SnH}$ units linked by Sn–Sn bonds, i.e. $(\text{Ar}^{\text{NiPr}_2}\text{Sn})_4\text{H}_2$ (**5**; Scheme 4). The molecular structure of **5** in the solid state was determined by X-ray crystallography (Figure 2). The tin-bound hydrides could be located in the difference Fourier map (and refined without restraints), and their presence confirmed by infra-red spectroscopy through an absorption at 1742 cm^{-1} . The stretching frequency is significantly blue-shifted relative to that of **4** (see below). The heavy atom skeleton of **5** resembles that of tetramer **1**, with the exception of a ca. 0.1 Å lengthening of the central Sn–Sn bond ($2.7762(3)\text{ Å}$ for **5**, cf. $2.6908(4)\text{ Å}$), consistent with a description in terms of a single bond between two tetravalent metal centres, rather than a two-way donor/acceptor double bond (for **1**). The Sn–N distances associated with the amine donors in **5** are consistent with a similar pattern of coordination behaviour as is observed in **4** (and **1**), i.e. effectively no coordination to the internal tin atoms Sn(2)/Sn(2'), and coordination of one of the amine donors to each terminal tin centre ($d(\text{Sn}(1)\cdots\text{N}(1)) = 2.425(2)\text{ Å}$). The solid-state ^{119}Sn NMR spectrum of **5** is characterized by two signals, one at -352 ppm assigned to Sn2/Sn2' (cf. -376 ppm (solution phase) for the internal tin centre in **4**), with a second resonance (at 510 ppm) due to the 'terminal' tin centres Sn1/Sn1'.

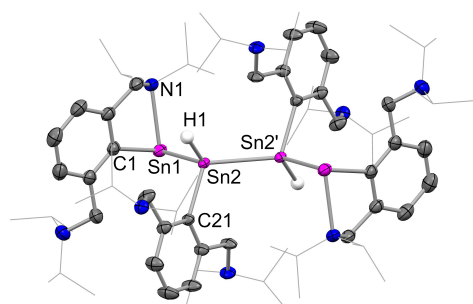


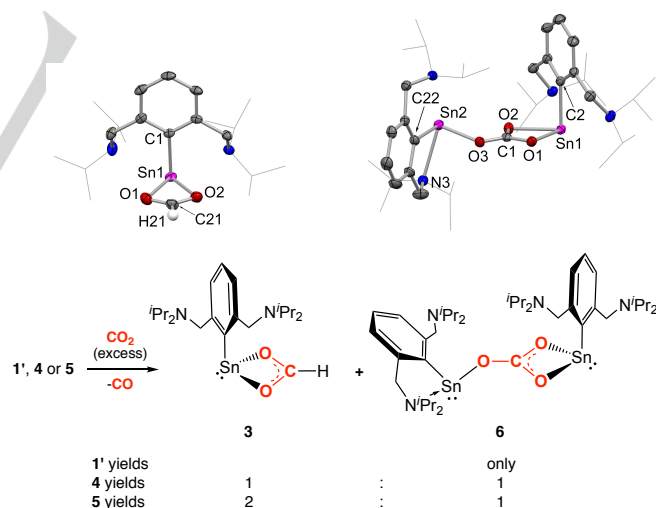
Figure 2. Molecular structure of $(\text{Ar}^{\text{NiPr}_2}\text{Sn})_4\text{H}_2$ (**5**) in the solid state as determined by X-ray crystallography. Solvent molecule and most hydrogen atoms omitted, and 'Pr groups shown in wireframe format for clarity. Thermal ellipsoids set at the 40 % probability level. Key bond lengths (Å): Sn1–C1 $2.194(3)$, Sn1–N1 $2.425(2)$, Sn1–Sn2 $2.866(1)$, Sn2–Sn2' $2.776(1)$, Sn2–C21 $2.190(3)$, Sn2–H1 $1.66(3)$. CCDC ref: 2094343.

From a structural perspective, related tri-/tetra-tin chains of the type $(\text{L}(\text{R}')\text{Sn}\{\text{Sn}(\text{H})(\text{R}')\})_n\text{Sn}(\text{R}')(\text{L})$ ($n = 1$, $\text{L} = \text{IMEt}_2$, $\text{R}' = 2,4,6\text{-triisopropylphenyl}$; $n = 2$, $\text{L} = \text{IMEt}_4$, $\text{R}' = \text{CH}(\text{SiMe}_3)_2$) have been reported by Wesemann and co-workers, although the synthetic route employed (NHC-mediated dehydrocoupling of stannanes, $\text{R}'\text{SnH}_3$), is distinct from the sequential chain growth employed here.^[24]

Most interestingly, the NMR spectra (^1H , ^{13}C and ^{119}Sn) of solutions formed by dissolving single crystals of **5** in benzene- d_6 reveal that the tetra-tin species reverts completely to a 1:1 mixture of hydride complex **2** and tri-tin chain **4** at room temperature under such conditions (Figures s14 and s15).^[25] The implication is that **5**, while stable in the solid state,

undergoes facile reductive elimination of $\text{Ar}^{\text{NiPr}_2}\text{SnH}$ in solution, implying that the Sn–H oxidative addition process which is proposed to give rise to **5** is in fact reversible. By means of comparison, the bis(boryl) stannylene $\text{Sn}\{\text{B}(\text{NDippCH})_2\}_2$ inserts into a range of E–H bonds ($\text{E} = \text{H}, \text{B}, \text{N}, \text{O}$ and Si), and the product of the oxidative addition of NH_3 (i.e. $\{(\text{HCDippN})_2\text{B}\}_2\text{Sn}(\text{NH}_2)\text{H}$), undergoes reductive elimination of $(\text{HCDippN})_2\text{B}(\text{NH}_2)$ and $(\text{HCDippN})_2\text{BH}$ over the course of several days at room temperature.^[26] In this case, the reductive elimination process is relatively slow. By contrast, the facile reductive elimination of a Sn–H bond from **5** (to yield **2** and **4**) implies a very low activation barrier for this process in solution. With this in mind, and with a view to further probing the chemical reversibility of the Sn–H bond activation processes giving rise to **4** and **5**, we examined their reactivity towards CO_2 .

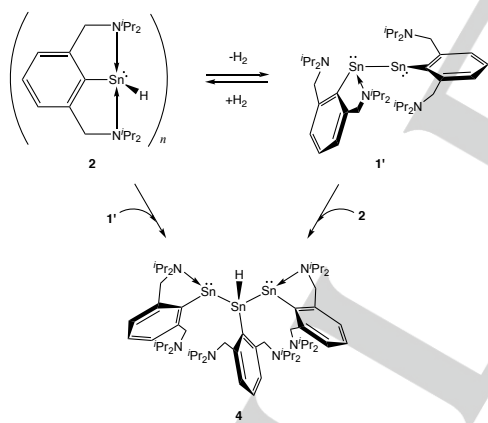
Tin(II) hydride (**2**) has been shown to react via insertion of CO_2 into the Sn–H bond to form the formate complex $\text{Ar}^{\text{NiPr}_2}\text{Sn}\{\kappa^2\text{-O}_2\text{CH}\}$ (**3**). As such, we hypothesised that the reaction of **5** with CO_2 could act as a further probe of the reversibility of Sn–H oxidative addition in the formation of the Sn_4 chain (Scheme 6). Formate **3** would be expected to be formed if the dissociation of **5** into **2** and **4** (as noted above) is facile under such reaction conditions. In the event, the reaction of **5** in benzene- d_6 with ca. 1 bar of CO_2 , generates a 2:1 mixture of **3** and the di-tin carbonate compound $(\text{Ar}^{\text{NiPr}_2}\text{Sn})_2(\text{O}_2\text{CO})$ (**6**; see below). The implication of the formation of two equivalents of **3** in this reaction is that **4** itself can act as a facile source of the tin hydride **2** via a second formal Sn–H reductive elimination step under these conditions. Consistently, the independent reaction of isolated **4** with CO_2 leads to the formation of **3** and **6** in a 1:1 ratio, implying that **4** does indeed act as a source of distannylene **1'** and hydride **2**.



Scheme 6. Formate and carbonate products formed in the reactions of mixed valence tin hydrides **4** and **5**, and distannylene **1'** with CO_2 . Molecular structures of $\text{Ar}^{\text{NiPr}_2}\text{Sn}\{\kappa^2\text{-O}_2\text{CH}\}$ (**3**) and $\text{Ar}^{\text{NiPr}_2}\text{Sn}_2\{\mu\text{-}\kappa^1(\text{O})\text{:}\kappa^2(\text{O},\text{O})\text{-CO}_2\}$ (**6**) in the solid state as determined by X-ray crystallography. Second component of asymmetric unit (for both **3** and **6**) and most hydrogen atoms omitted, and 'Pr groups shown in wireframe format for clarity. Thermal ellipsoids set at the 40 % probability level. Key bond lengths (Å): (for **3**) Sn1–C1 $2.177(3)$, Sn1 $\cdots\text{N}$ $2.789(3)$, $2.861(3)$, Sn1–O $2.356(3)$, $2.386(3)$, C21–O $1.223(6)$, $1.251(5)$; (for **6**) Sn1–C2 $2.194(4)$, Sn1 $\cdots\text{N}$ $2.897(5)$, $2.926(6)$, Sn1–O $2.327(2)$, $2.256(3)$, C1–O1 $1.283(5)$, C1–O2 $1.280(6)$, C1–O3 $1.303(5)$, Sn2–O $2.144(3)$, Sn1 $\cdots\text{N}$ $2.538(3)$, $2.813(3)$. CCDC refs: 2094341 and 2094344.

The fact that the carbonate component of the product mixture (i.e. **6**) is derived from distannyne **1'** was verified by its independent reaction with CO₂. **6** can also be synthesised via the reaction of Ar^{NiPr₂}SnHal and Cs₂CO₃ in THF, and has been characterised by standard spectroscopic/analytical techniques, and X-ray crystallography (Scheme 6). The formation of **6** from **1'** (or from **4/5**) proceeds via reduction of one equivalent of CO₂ to CO. A small number of examples of the digermynes-mediated reduction of carbon dioxide have been reported;^[27,28] in these cases a bis(germylene)oxide complex is typically isolated as the metal-containing product. **1'** is, to the best of our knowledge, the first example of a distannyne which effects reduction of carbon dioxide. We propose that the reduction of CO₂ by **1'** initially forms the bis(stannylyne)oxide complex (Ar^{NiPr₂}Sn)₂O (as in the related digermynes chemistry), which then inserts a second equivalent of CO₂ to yield the carbonate product, **6**.

Finally, the possibility for reversible oxidative addition of the Sn–H bond of **2** at one/both tin centres of **1'** also provides a rationale for two further observations regarding hydrogenation/dehydrogenation chemistry (Scheme 7). Firstly, prolonged storage of tin(II) hydride **2** in hexane solution leads to the evolution of H₂ and to the formation of tetra-tin system **5** (in the solid state) or tri-tin system **4** (in solution). In the reverse sense, the reaction of distannyne **1'** with dihydrogen (at ca. 1 atm pressure) in benzene-d₆ solution leads to the formation of **4**. Both observations are consistent with the idea of facile inter-conversion between **1'** and **2** (depending on the presence or otherwise of H₂),^[5h] and with the mixtures of **1'** and **2** so generated then yielding **4** (in solution) or **5** (in the solid state) - via the Sn–H oxidative addition steps demonstrated explicitly in stoichiometrically controlled reactions (Scheme 4).



Scheme 7. Solution-phase dehydrogenation of **2**/hydrogenation of **1'** leading to the formation of **4**.

Conclusions

We have shown that a distannyne featuring hemi-labile pendant NⁱPr₂ groups can (i) reversibly catenate via Sn=Sn bond formation; and (ii) undergo Sn–H oxidative addition at one/both tin centres to generate mixed-valence tri- and tetra-tin chain containing internal –Sn(Ar)H– units and terminal base-stabilized stannylyne functions. Of interest from a reactivity perspective are the observations that (i) oxidative addition of a Sn–H bond at one tin centre in distannyne **1'** generates (in **4**) a tri-tin product which is stable in the solid state and undergoes ca. 13 %

reversion to **1'**/2 in solution; while (ii) the corresponding tetra-tin system **5**, formed via two oxidative addition steps, is seen only in the solid state and undergoes *complete* Sn–H reductive elimination in solution; and (iii) no hint of further chain growth at the stannylyne termini of **5** is seen in any experiments. These observations hint at decreasing ease of Sn–H oxidative addition as the chain gets longer. In the cases of **4** and **5**, this is consistent with the Sn–N distances measured in the solid state (2.645(6)/2.604(4) and 2.425(2) Å, respectively) which imply that the donor/acceptor interaction involving the amine donor becomes stronger (and less labile) as the tin chain lengthens. These metrical data are also consistent with the measured ¹¹⁹Sn chemical shifts for the stannylyne termini of **4** and **5** (δ_{Sn} = 629 and 510 ppm, respectively) which imply enhanced coordination of the hemi-labile N-donor for the latter.^[18] Although no structural data is available for the distannyne **1'** (due to its dimerization to give tetrameric **1** in the solid state), it is informative that its ¹¹⁹Sn chemical shift in solution (974 ppm) is at even lower field than that of **4** - implying even weaker interaction with the pendant N-donors on the NMR timescale. The minimum energy structure calculated for **1'** (at the PBE1PBE-GD3BJ/Def2-TZVP level) is unsymmetrical, with one of the tin centres featuring no Sn–N contacts shorter than 4 Å. As such, both the NMR and quantum chemical data for **1'** imply relatively facile access to an essentially two-coordinate tin centre, consistent with the ready oxidative addition chemistry observed experimentally for **1'**.

We hypothesize that the tighter binding of the pendant amine donor functions at the terminal tin centres on going from **1'** to **4** to **5** is influenced by the number of intervening –Sn(Ar)H– units (which increases from 0 to 1 to 2). These tetravalent (higher formal oxidation state) Sn centres effectively exert an electron-withdrawing effect on the stannylyne termini, rendering them more electrophilic and thereby drawing in the pendant amine donors. As such, the terminal tin centres are less liable to oxidative addition from both thermodynamic (less electron rich) and kinetic perspectives (tighter amine binding) as the chain length increases. The fact that the –Sn(Ar)H– function acts, in effect, as an electron-withdrawing group is reflected in the markedly different Sn–H stretching frequencies measured by IR spectroscopy for **4** and **5** (1644 and 1742 cm^{–1}, respectively). In **4** the tin atom bearing the Sn–H bond is flanked by two stannylyne functions, while in **5**, the corresponding unit is flanked by one such divalent tin centre and an electron-withdrawing tetravalent function. The shifting of IR stretches to higher frequencies in the presence of electron-withdrawing groups is well precedented.^[29,30]

Acknowledgements

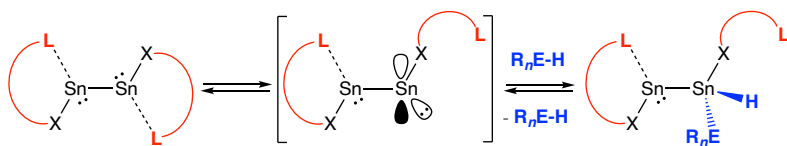
We thank the Leverhulme Trust and EPSRC for funding. PV would like to thank the Academy of Finland for financial support (project number 314794) and Prof. Heikki M. Tuononen for providing computational resources.

Keywords: tin • oxidative addition • reductive elimination • hemi-labile ligand • reversibility

- [1] See, for example: J. F. Hartwig, *Organotransition Metal Chemistry: From Bonding to Catalysis*; University Science Books, Sausalito, CA, 2010.
- [2] See for example: a) N. L. Dunn, M. Ha, A. T. Radosevich, *J. Am. Chem. Soc.* **2012**, *134*, 11330–11333; b) O. Planas, F. Wang, M. Leutzsch, J. Cornella, *Science* **2020**, *367*, 313–317.
- [3] For a broad-ranging comparative discussion of Main Group elements and Transition Metals see: a) P. P. Power, *Nature* **2010**, *463*, 171–177. See also: b) C. Weetman, S. Inoue, *ChemCatChem* **2018**, *10*, 4213–4228.
- [4] For reviews of the reactivity of singlet carbenes/heavier metallocene see, for example: a) D. Martin, M. Soleilhavoup, G. Bertrand, *Chem. Sci.* **2011**, *2*, 389–399. See also b) Y. Mizuhata, T. Sasamori, N. Tokitoh, *Chem. Rev.* **2009**, *109*, 3479–3511; c) S. Yao, Y. Xiong, M. Driess, *Organometallics* **2011**, *30*, 1748–1767; d) T. Chu, G. I. Nikonov, *Chem. Rev.* **2018**, *118*, 3608–3680.
- [5] For reversible E–H bond activation at main group element centres, see for example: a) J. P. Moerdyk, G. A. Blake, D. T. Chaes, C. W. Bielawski, *J. Am. Chem. Soc.* **2013**, *135*, 18798–18801; b) C. Ganesamoorthy, S. Loerke, C. Gemel, P. Jerabek, M. Winter, G. Frenking, R. A. Fischer, *Chem. Commun.* **2013**, *49*, 2858–2860; c) T. Chu, I. Korobkov, G. I. Nikonov, *J. Am. Chem. Soc.* **2014**, *136*, 9195–9202; d) K. Inomata, T. Watanabe, Y. Miyazaki, H. Tobita, *J. Am. Chem. Soc.* **2015**, *137*, 11935–11937; e) R. Rodriguez, Y. Contie, Y. Mao, N. Saffon-Merceron, A. Baceiredo, V. Branchadell, T. Kato, *Angew. Chem. Int. Ed.* **2015**, *54*, 15276–15279; f) R. Rodriguez, Y. Contie, R. Nougé, A. Baceiredo, N. Saffon-Merceron, J.-M. Sotiropoulos, T. Kato, *Angew. Chem. Int. Ed.* **2016**, *55*, 14355–14358; g) S. Unwin, D. M. Rogers, G. S. Nichol, M. J. Cowley, *Dalton Trans.* **2016**, *45*, 13695–13699; h) S. Wang, T. J. Sherbow, L. A. Berben, P. P. Power, *J. Am. Chem. Soc.* **2018**, *140*, 590–593; i) R. C. Turnell-Ritson, J. S. Sapsford, R. T. Cooper, S. S. Lee, T. Földes, P. A. Hunt, I. Pápai, A. E. Ashley, *Chem. Sci.* **2018**, *9*, 8716–8722; j) R. S. Falconer, G. S. Nichol, I. V. Smolyar, S. L. Cockroft, M. J. Cowley, *Angew. Chem. Int. Ed.* **2020**, *60*, 2047–2052.
- [6] For other reversible small molecule activation processes occurring at main group element centres see, for example: a) Y. Peng, B. D. Ellis, X. Wang, J. C. Fetting, P. P. Power, *Science* **2009**, *325*, 1668–1670; b) R. Rodriguez, D. Gau, T. Kato, N. Saffon-Merceron, A. De Cózar, F. P. Cossio, A. Baceiredo, *Angew. Chem. Int. Ed.* **2011**, *50*, 10414–10416; c) F. Lips, J. C. Fetting, A. Mansikkamäki, H. M. Tuononen, P. P. Power, *J. Am. Chem. Soc.* **2013**, *136*, 634–637; d) A. V. Protchenko, D. Dange, M. P. Blake, A. D. Schwarz, C. Jones, P. Mountford, S. Aldridge, *J. Am. Chem. Soc.* **2014**, *136*, 10902–10905; e) J. W. Dube, C. M. E. Graham, C. L. B. Macdonald, Z. D. Brown, P. P. Power, P. J. Ragogna, *Chem.-Eur. J.* **2014**, *20*, 6739–6744; f) J. D. Eickson, J. C. Fetting, P. P. Power, *Inorg. Chem.* **2015**, *54*, 1940–1948; g) J. Hicks, P. Vasko, J. M. Goicoechea, S. Aldridge, *J. Am. Chem. Soc.* **2019**, *141*, 11000–11003; h) C. Bakewell, A. J. P. White, M. R. Crimmin, *Chem. Sci.* **2019**, *10*, 2452–2458; i) C. Bakewell, M. Garçon, R. Y. Kong, L. O'Hare, A. J. P. White, M. R. Crimmin, *Inorg. Chem.* **2020**, *59*, 4608–4616.
- [7] A. Caise, L. P. Griffin, A. Heilmann, C. McManus, J. Campos, S. Aldridge, *Angew. Chem. Int. Ed.* **2021**, in press (DOI: 10.1002/anie.202104643).
- [8] a) P. J. Davidson, D. H. Harris and M. F. Lappert, *J. Chem. Soc., Dalton Trans.* **1976**, *21*, 2268–2274; b) D. E. Goldberg, D. H. Harris, M. F. Lappert and K. M. Thomas, *J. Chem. Soc., Chem. Commun.* **1976**, 261–262.
- [9] a) K. Tamao, K. Nagata, M. Asahara, A. Kawachi, Y. Ito, M. Shiro, *J. Am. Chem. Soc.* **1995**, *117*, 11592–11593; (b) A. Toshimitsu, S. Hirao, T. Saeki, M. Asahara, K. Tamao, *Heteroatom Chem.* **2001**, *12*, 392–397.
- [10] Lithiation of 2,6-(¹Pr₂NCH₂)₂C₆H₃Br followed by reaction with SnCl₂ gives a crystalline material formulated as Ar^{NiPr₂}SnCl_{0.6}Br_{0.4} (based on ¹¹⁹Sn NMR data), which can be used for further reaction chemistry. Ar^{NiPr₂}SnBr can be prepared selectively by using SnBr₂ instead of SnCl₂, and Ar^{NiPr₂}SnI then synthesized from the bromide via reaction with Me₃SiI (see ESI for synthetic details).
- [11] S. P. Green, C. Jones, A. Stasch, *Science*, **2007**, *318*, 1754–1757.
- [12] M. Novák, M. Bouška, L. Dostál, A. Růžicka, A. Hoffmann, S. Herres-Pawlis, R. Jambor, *Chem. - A Eur. J.* **2015**, *21*, 7820–7829.
- [13] R. Jambor, B. Kašná, K. N. Kirschner, M. Schürmann, K. Jurkschat, *Angew. Chem. - Int. Ed.* **2008**, *47*, 1650–1653.
- [14] S. Khan, R. Michel, J. M. Dieterich, R. A. Mata, H. W. Roesky, J. P. Demers, A. Lange, D. Stalke, *J. Am. Chem. Soc.* **2011**, *133*, 17889–17894.
- [15] V. Y. Lee, T. Fukawa, M. Nakamoto, A. Sekiguchi, B. L. Tumanskii, M. Karni, Y. Apeloig, *J. Am. Chem. Soc.* **2006**, *128*, 11643–11651.
- [16] A. D. Phillips, R. J. Wright, M. M. Olmstead, P. P. Power, *J. Am. Chem. Soc.* **2002**, *124*, 5930–5931.
- [17] B. E. Eichler, B. L. Phillips, P. P. Power, M. P. Augustine, *Inorg. Chem.* **2000**, *39*, 5450–5453.
- [18] a) B. Wrackmeyer in *Tin Chemistry. Fundamentals, Frontiers and Applications* (Eds.: A. G. Davies, M. Gielen, K. H. Pannel, E. R. T. Tiekink), Wiley, Chichester, 2008, pp. 17 – 52. For recent examples relating to the coordination of weak additional donors at tin see, for example: b) J. Li, C. Schenk, F. Winter, H. Scherer, N. Trapp, A. Higelin, S. Keller, R. Pöttgen, I. Krossing, C. Jones, *Angew. Chem. Int. Ed.* **2012**, *51*, 9557–9561; c) C. P. Sindlinger, F. S. W. Aicher, L. Wesemann, *Inorg. Chem.* **2017**, *56*, 548–560.
- [19] For a related example of E–H reductive elimination at tin, see: a) F. Diab, F. S. W. Aicher, C. P. Sindlinger, K. Eichele, H. Schubert, L. Wesemann, *Chem.-Eur. J.* **2019**, *25*, 4426–4434. See also: b) C. P. Sindlinger, L. Wesemann, *Chem. Sci.* **2014**, *5*, 2739 –2746; c) C. P. Sindlinger, A. Stasch, H. F. Bettinger, L. Wesemann, *Chem. Sci.* **2015**, *6*, 4737–4751; d) C. P. Sindlinger, W. Grahneis, F. S. W. Aicher, L. Wesemann, *Chem. Eur. J.* **2016**, *22*, 7554–7566; e) C. P. Sindlinger, F. S. W. Aicher, H. Schubert, L. Wesemann, *Angew. Chem. Int. Ed.* **2017**, *56*, 2198 –2202.
- [20] L. W. Pineda, V. Jancik, K. Starke, R. B. Oswald, H. W. Roesky, *Angew. Chem. - Int. Ed.* **2006**, *45*, 2602–2605.
- [21] S. Khan, P. P. Samuel, R. Michel, J. M. Dieterich, R. a. Mata, J.-P. Demers, A. Lange, H. W. Roesky, D. Stalke, *Chem. Commun.* **2012**, *48*, 4890.
- [22] A. Jana, H. W. Roesky, C. Schulzke, A. Döring, *Angew. Chemie - Int. Ed.* **2009**, *48*, 1106–1109.
- [23] T. J. Hadlington, C. E. Kefalidis, L. Maron, C. Jones, *ACS Catal.* **2017**, *7*, 1853–1859.
- [24] J. J. Maudrich, C. P. Sindlinger, F. S. W. Aicher, K. Eichele, H. Schubert, L. Wesemann, *Chem. - A Eur. J.* **2017**, *23*, 2192–2200.
- [25] Cooling such a solution comprised of equimolar quantities of **2/4** to ca. 190 K does lead to the appearance of additional signals in the ¹H NMR spectrum of the mixture, although given the broadness of the spectrum it is difficult to ascertain whether these arise from the formation of **5** at low temperatures, or from the slowing of fluxional processes associated with **2/4**. Low temperature ¹¹⁹Sn NMR is also hampered by significant signal broadening below 243 K.
- [26] A. V. Protchenko, J. I. Bates, L. M. A. Saleh, M. P. Blake, A. D. Schwarz, E. L. Kolychev, A. L. Thompson, C. Jones, P. Mountford, S. Aldridge, *J. Am. Chem. Soc.* **2016**, *138*, 4555–4564.
- [27] J. Li, M. Hermann, G. Frenking, C. Jones, *Angew. Chemie - Int. Ed.* **2012**, *51*, 8611–8614.
- [28] J. A. Kelly, M. Juckel, T. J. Hadlington, I. Fernández, G. Frenking, C. Jones, *Chem. - A Eur. J.* **2019**, *25*, 2773–2785.
- [29] See, for example: A. Caise, D. Jones, E. L. Kolychev, J. Hicks, J. M. Goicoechea, S. Aldridge, *Chem.-Eur. J.* **2018**, *24*, 13624–13635.
- [30] Deposition Numbers 2094340, 2094341, 2094342, 2094343, 2094344, 2094345 and 2094346 contain the supplementary crystallographic data for this paper. These data are provided free of charge by the joint Cambridge Crystallographic Data Centre and Fachinformationszentrum Karlsruhe Access Structures service www.ccdc.cam.ac.uk/structures.

Entry for the Table of Contents

Insert graphic for Table of Contents here.



Reversible bond activation mediated by (de)coordination of a hemi-labile donor, **L**

Insert text for Table of Contents here. (392 characters)

We report a distannylene supported by a pincer ligand featuring pendant $\text{CH}_2\text{N}^i\text{Pr}_2$ arms that is capable of reversibly activating E–H bonds at one or both of the tin centres through dissociation of the hemi-labile N–Sn donor/acceptor interactions. This chemistry can be exploited to sequentially (and reversibly) assemble mixed-valence chains of tin atoms of the type $\text{ArSn}\{\text{Sn}(\text{Ar})\text{H}\}_n\text{SnAr}$ ($n = 1, 2$).

Institute and/or researcher Twitter usernames: [@GroupAldridge](#)